Validating a Hot VDE in C-Mod with M3D-*C*[1]

C. Clauser[1], R. Sweeney[2], R. Granetz[1], A. Kumar[1], N. Ferraro[3], and S. Jardin[3]

[1] Plasma Science and Fusion Center | MIT
[2] Commonwealth Fusion Systems
[3] Princeton Plasma Physics Laboratory

Acknowledgments:
J. Chen (PPPL)
E. S. Seol (RPI)

M3D-C^1 is becoming a valuable tool to help inform SPARC and ARC physics/design

- M3D-C^1 is an X-MHD code that includes resistive walls and as well as other disruption-relevant capabilities (impurities, runaways, particle pusher, etc).
  - On VDE physics: 2D and 3D benchmarks with NIMROD and JOREK were conducted [Krebs PoP2020, Artola PoP2021].

- However, validation with experiments remains a critical step to continue improving the modeling and to build confidence on projected quantities for SPARC/ARC/ITER and future devices.
  - **A critical question is whether 2D simulations can capture overall plasma dynamics and halo currents properly with realistic assumptions.**

- **C-Mod offers a unique opportunity with comprehensive hot and cold VDE data.**

Outline

- **Overview of C-Mod experimental results for a hot VDE (#950111006)**
- **2D Hot VDE modeling with M3D-*C*^{1}**
- **Comparison with the experiment (Validation)**
- **Summary**

Experiments in Alcator C-Mod were equipped with sensors to diagnose VDE and halo current dynamics

- Halo currents were diagnosed with various set of Rogowski coils that encircled the entire inner wall

- Current density centroid was tracked by
  - x-ray emission
  - filament reconstruction from magnetic signals

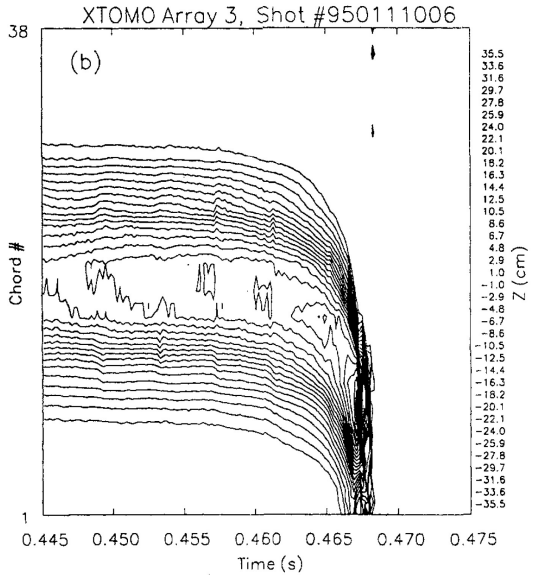

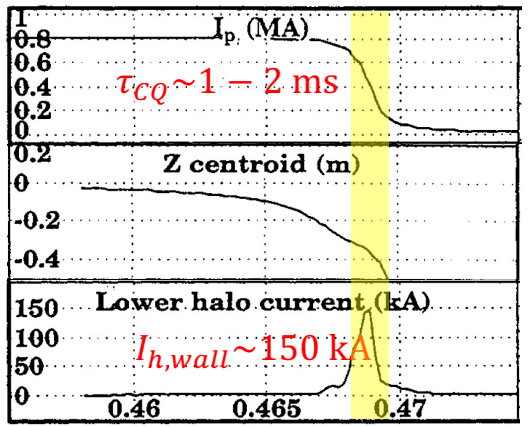

Flux from filament reconstruction, and halo current path

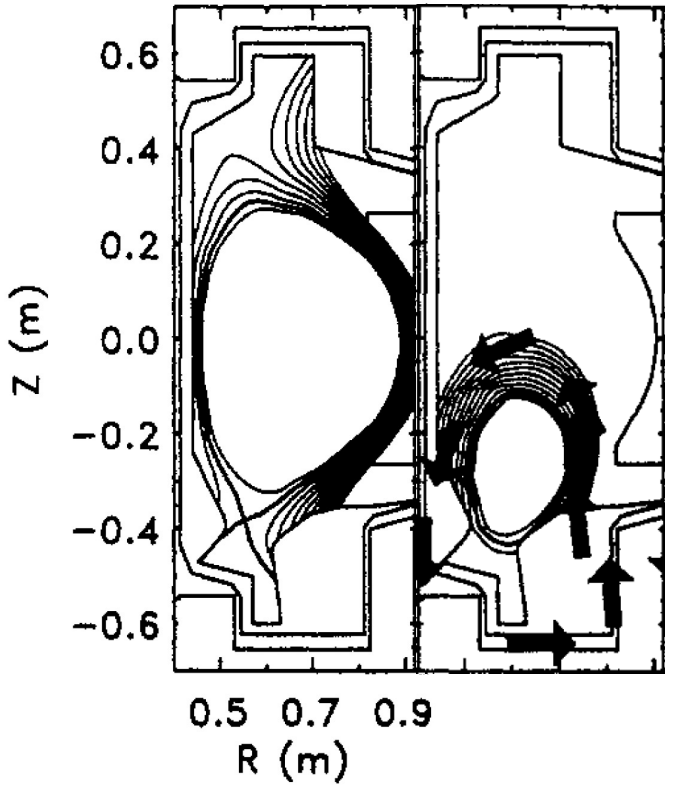

R. Granetz et al., Nucl. Fusion **36** (1996) 548

Present Limitations in the Modeling Capabilities can Challenge the Validation Exercise

Coil currents change during the VDE

Coil currents (A)

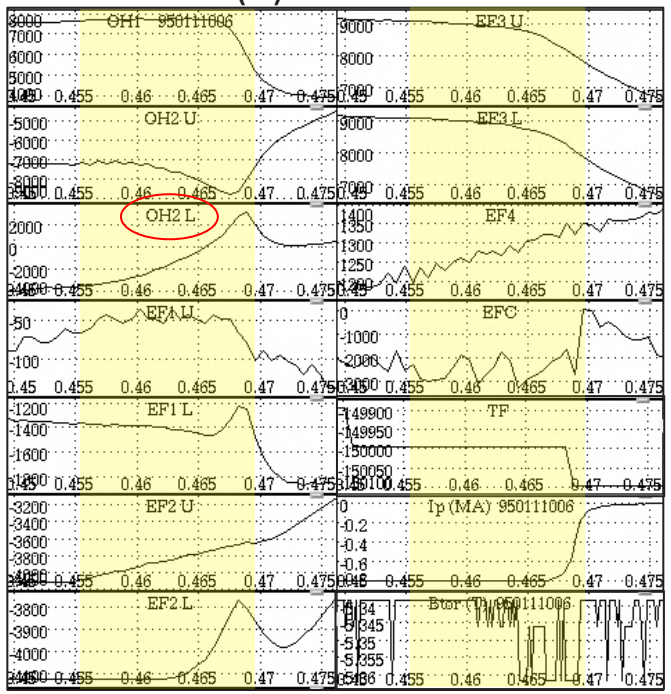

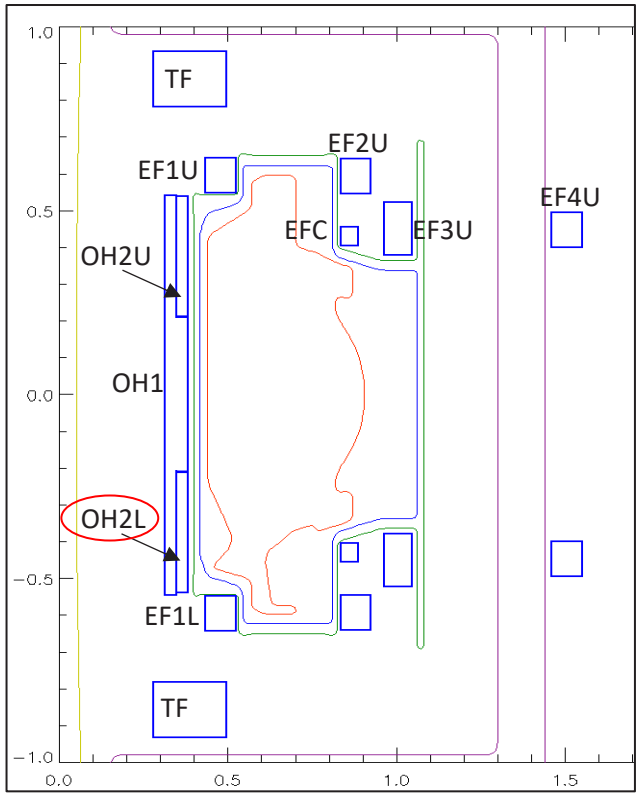

Last EFIT reconstruction at 0.46 s

EFIT equilibrium used was at 0.44 s

Realistic poloidal wall resistivity paths are complex

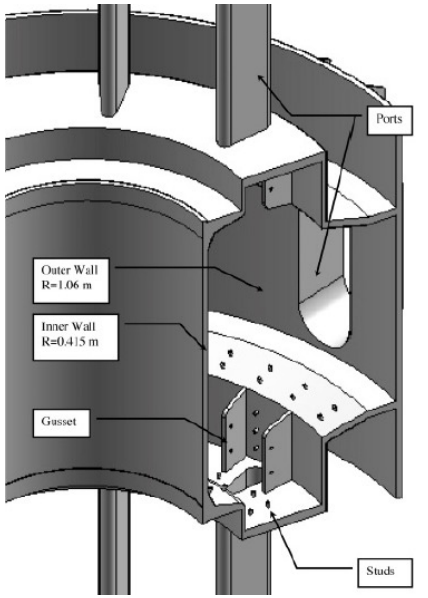

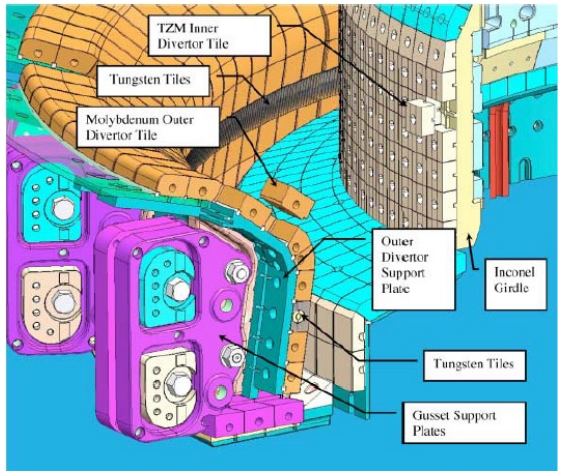

J. Irby et al., Fusion Sci. Tech. **51** (2007) 460

In this validation exercise we employed a uniform poloidal wall resistivity

C-Mod massive dome and cylinder structures do not play a significant role over disruption time scales

Different C-Mod models were generated, and L/R tests were conducted

C-Mod has (actually had)

- a stainless-steel vacuum vessel (304L, $\eta = 7\times10^{-7}$ Ωm) and
- a 'massive' dome/cylinder stainless-steel structure (316LN, $\eta = 7.4\times10^{-7}$ Ωm)

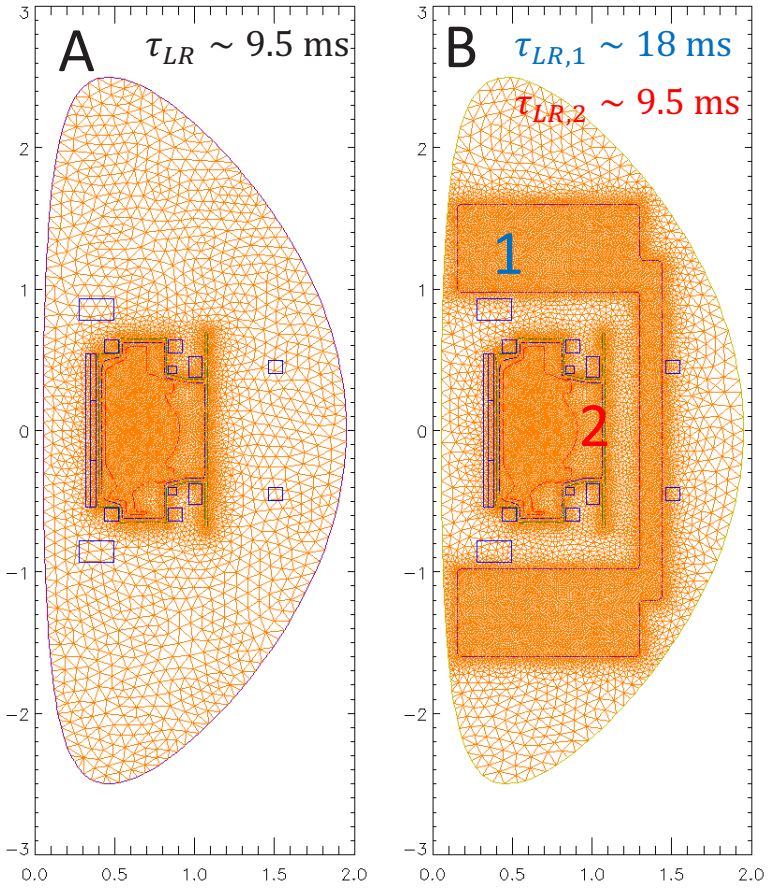

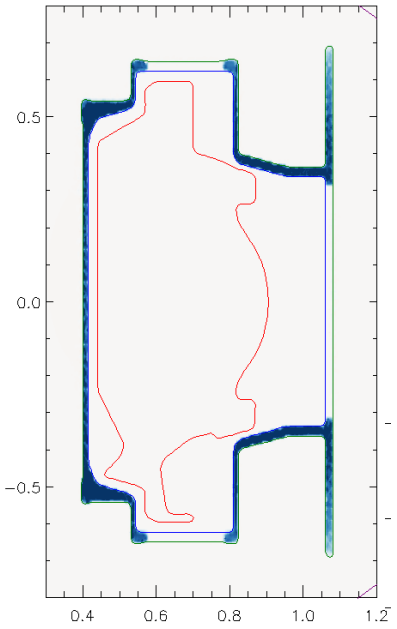

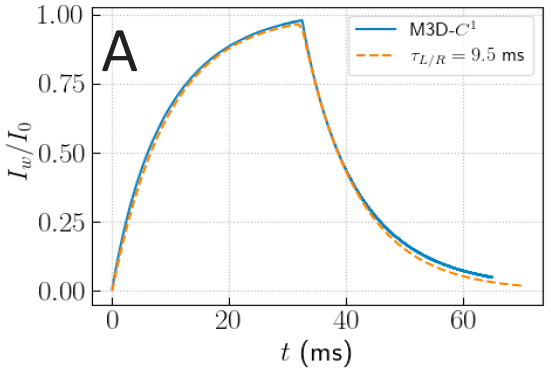

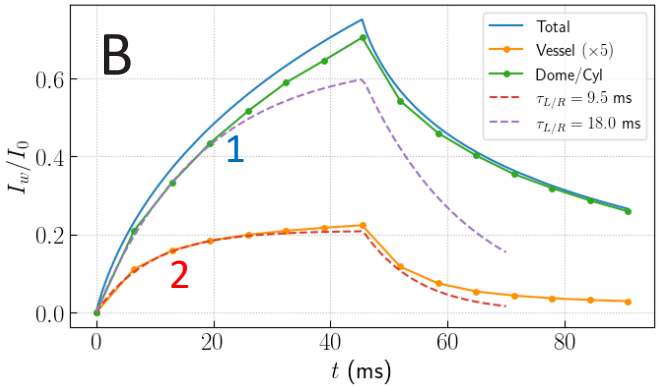

VDE evolved until edge safety factor fell below 2 without forcing a thermal quench

- A. wall contact occurs leading to an increase in the plasma current
- B. At $q_{95} \lesssim 2$. Skin currents develop, likely leading to 3D instabilities

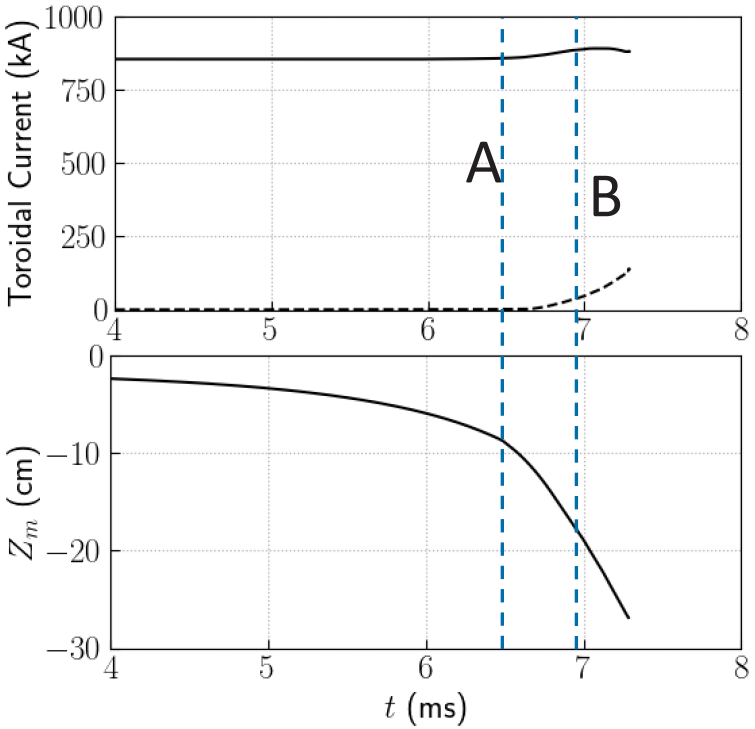

A. wall contact

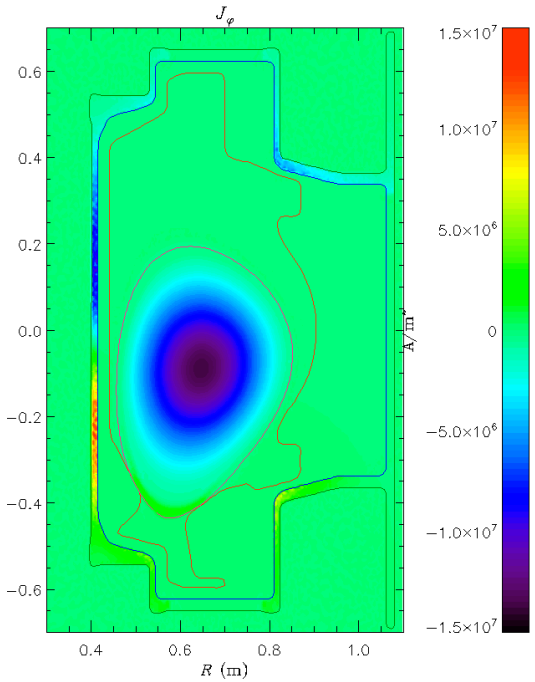

B. $q_{95} \lesssim 2$

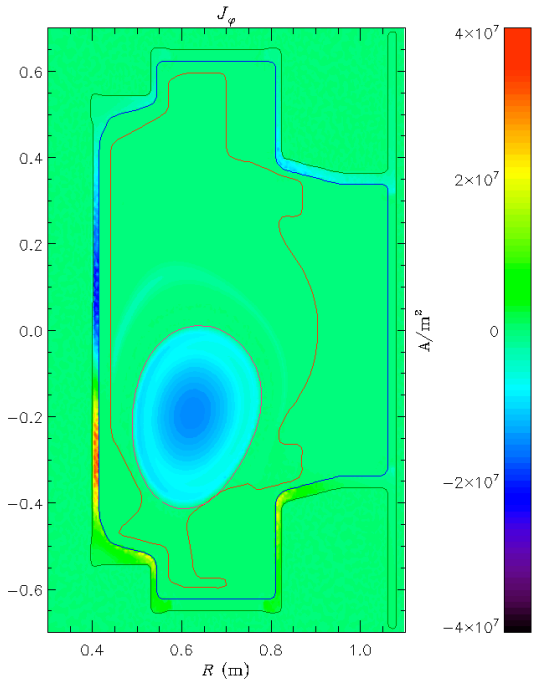

If thermal diffusivity is not increased after the plasma touches the wall, simulation suggests TQ should likely occur after $q_{95} \sim 2$

TQ induced at $q_{95} \approx 2$ and scanning over post-TQ and boundary temperatures to assess the CQ timescale

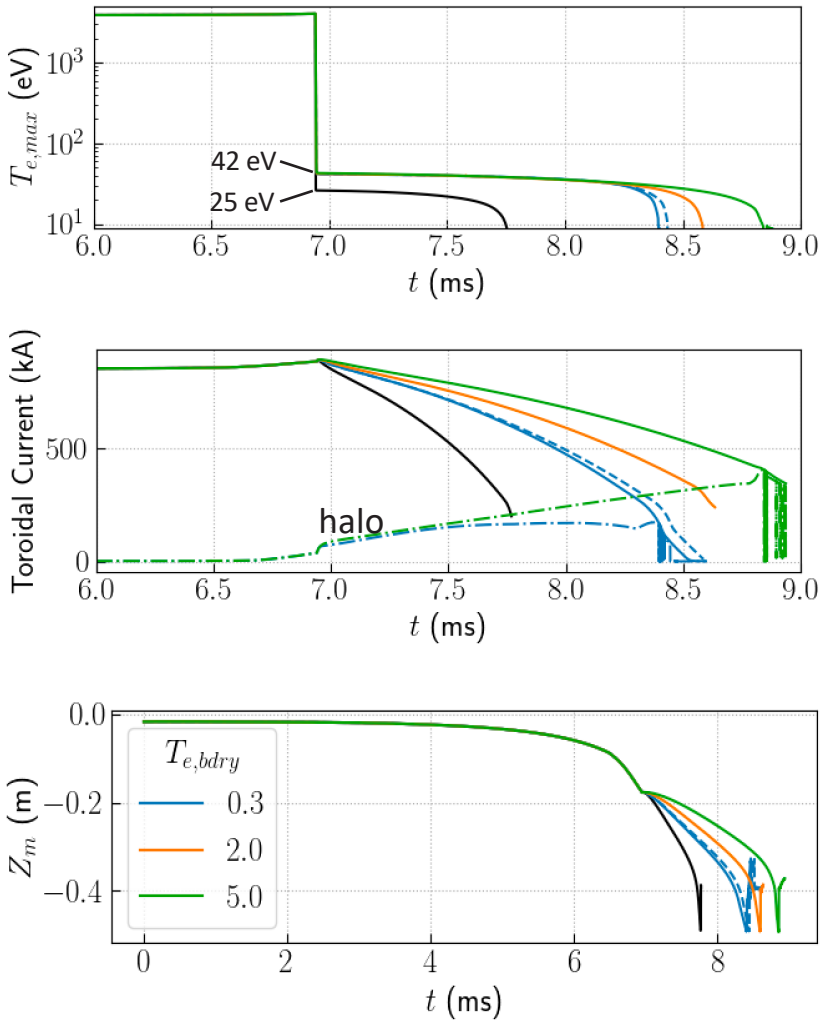

- Thermal diffusivity increased, so that post-TQ T_e fell to 42 and 25 eV
- Boundary Temperatures of 0.3, 2 and 5 eV were chosen, to cover a broad range.

- Both post-TQ and boundary T_e have a significant impact on
  - the CQ duration, τ_{CQ}
  - the vertical motion

  through the formation of halo currents

A post-TQ $T_e \sim 40$ eV is consistent with the experimental $\tau_{CQ} \sim 1 - 2$ ms

First comparison with experiment leads to agreements and disagreements

Simulations' time evolution were offset to match CQ with experiment

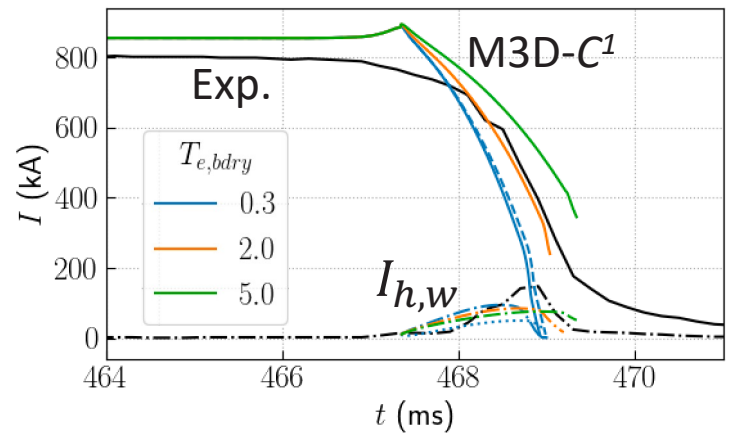

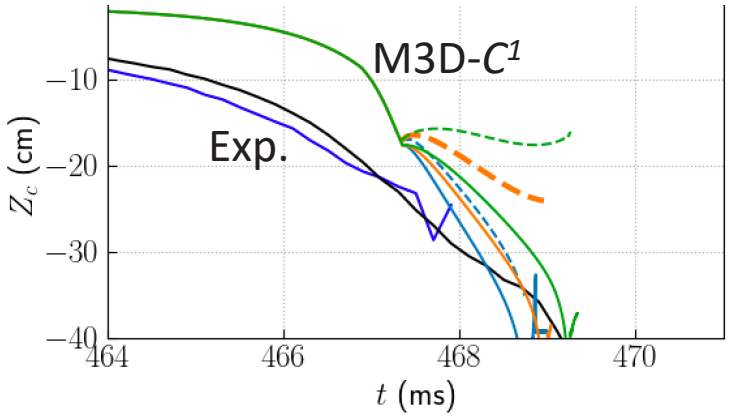

- ✓ Right CQ time scale for a post-TQ plasma of ~40 eV consistent with experiments
- ✗ Current spike not observed in the experiment, which suggest thermal diffusion increases after plasma contact
- ✓ Poloidal wall halo current ($I_{h,w}$) magnitude of ~100 kA in good agreement with experiment (~150 kA)
- ✗ Pre-TQ vertical motion does not agree well
- ✓ 2 eV boundary temperature gives the right displacement rate of the current density centroid

Examples of poloidal halo current patterns

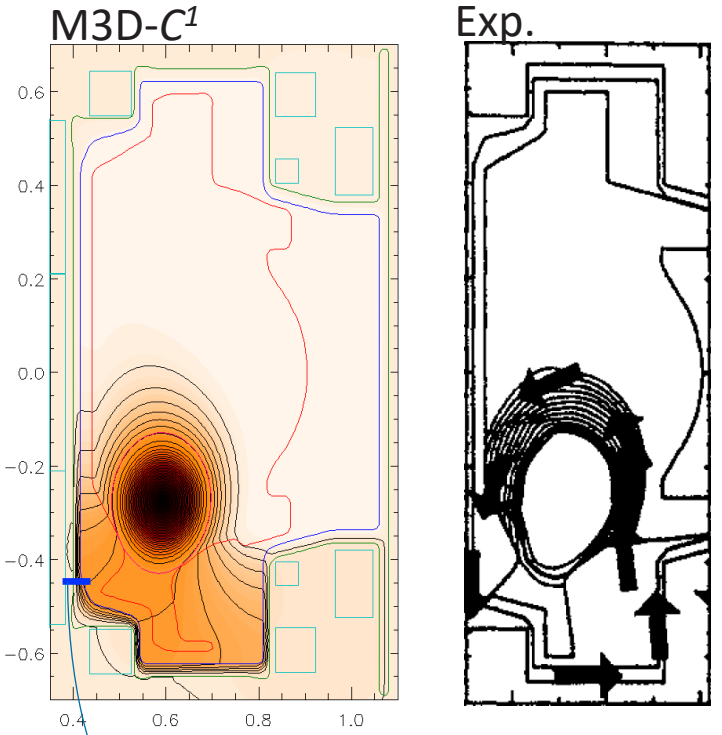

New simulations adjusting thermal conductivity and with 2 eV boundary temperature agree better with experiment

- Thermal conductivity was gradually increased after plasma contact to avoid current spike.
- Two simulations show TQ initiated at $q_{95} \sim 2$ and $q_{95} \sim 1$ suggest full TQ is triggered at this later stage

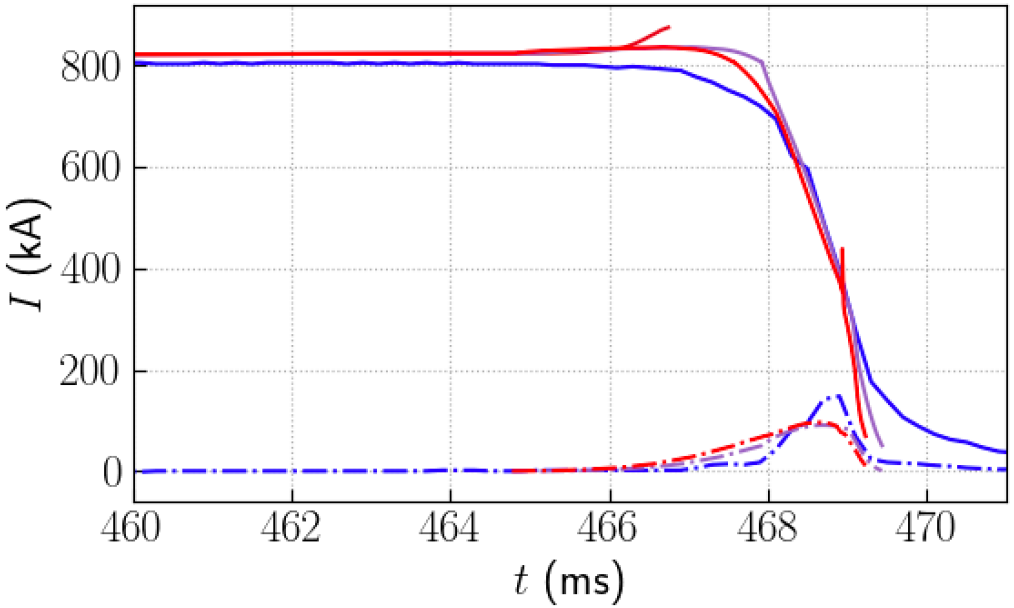

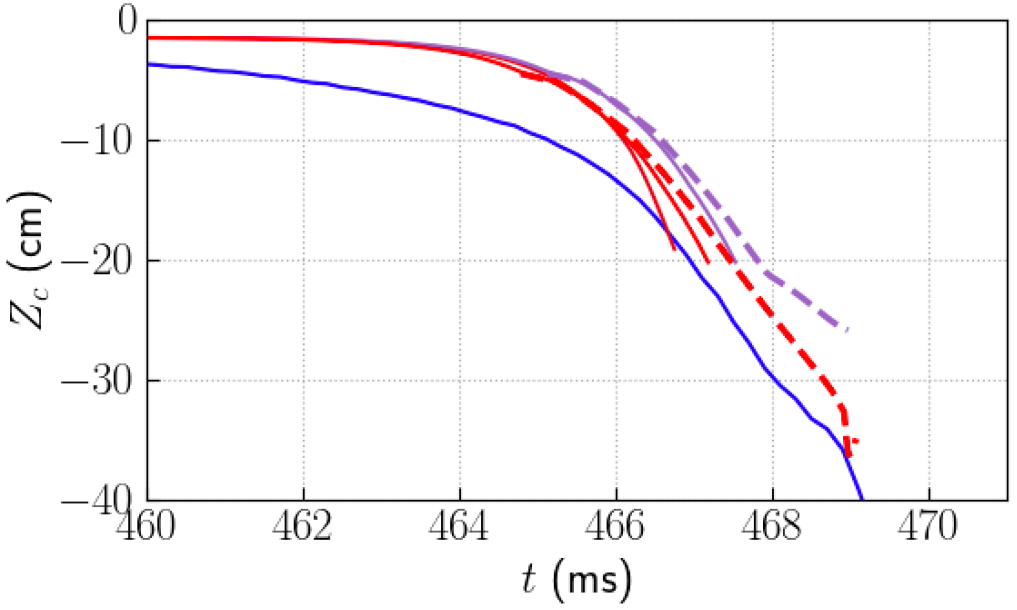

The mismatch at the early phase of the VDE might be likely due to dynamic coil currents present in the experiment

Summary

Validation of a hot VDE in C-Mod was conducted with M3D-*C*^{1}

- Good agreement was obtained with realistic modeling assumptions.
- This provides confidence on ongoing projections on SPARC and ARC.

Simulations suggest:

- Thermal conductivity increases when plasma becomes limited.

- Full thermal quench likely to occur when $q_{95} \sim 1$ rather than $q_{95} \sim 2$.

- Plasma halo currents play an important role during the VDE, affecting the current density centroid.

Remaining discrepancies at early phase might be due to static coil currents and simplified poloidal resistivity model in the code and will be explored in the future (Other effects?).

Extra slides

C-Mod massive dome and cylinder structures do not play a significant role over disruption time scales

Different C-Mod models were generated, and L/R tests were conducted

C-Mod has (actually had)

- a stainless-steel vacuum vessel (304L, $\eta = 7\times10^{-7}$ Ωm) and
- a 'massive' dome/cylinder stainless-steel structure (316LN, $\eta = 7.4\times10^{-7}$ Ωm)

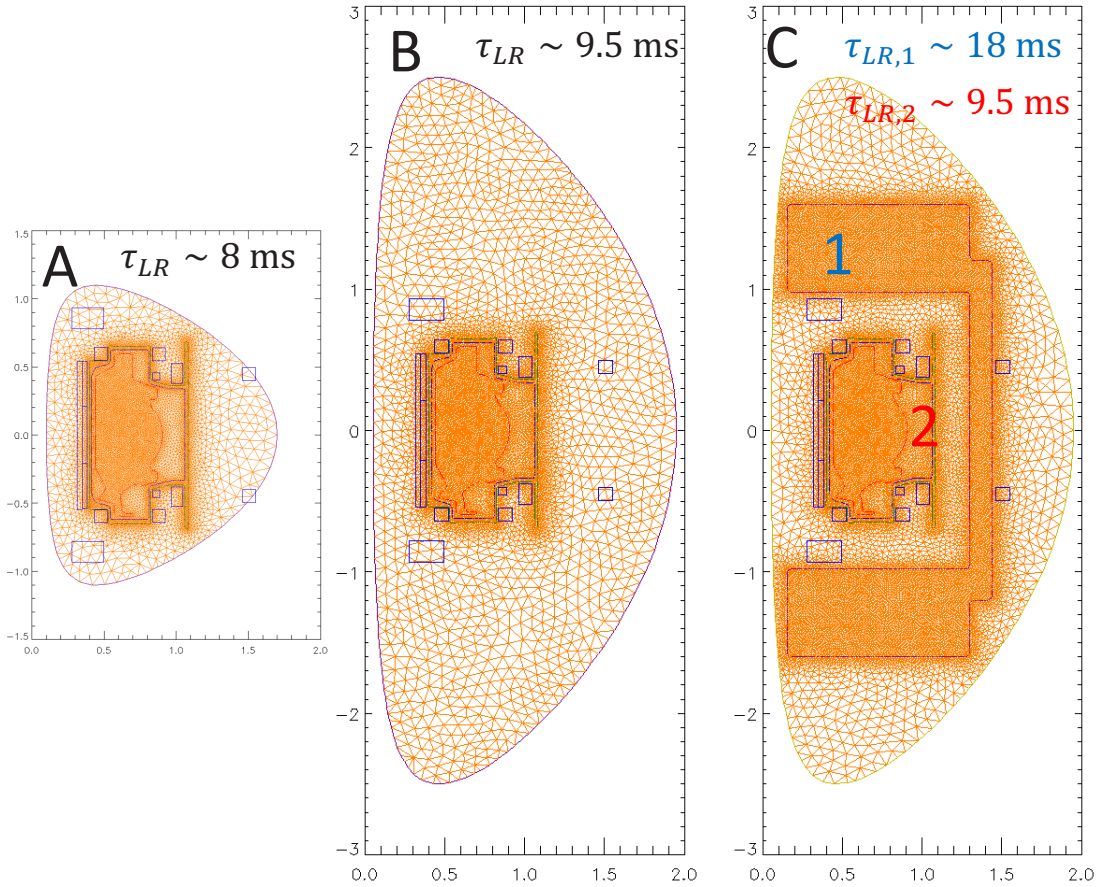

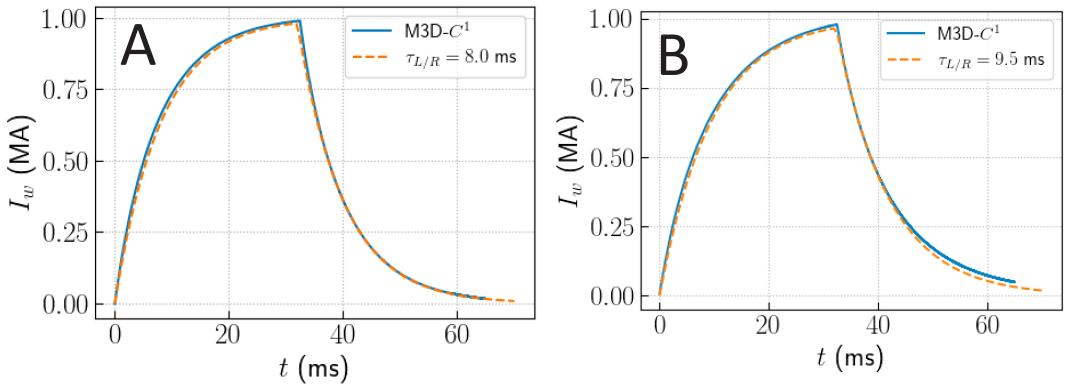

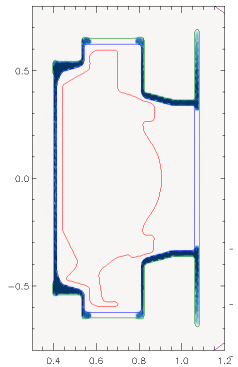

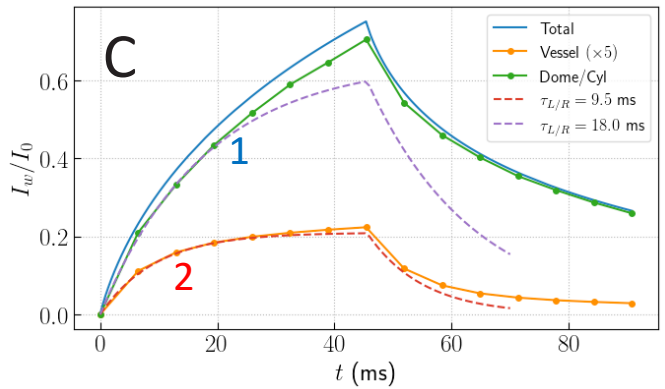

Vertical Displacement Events were conducted to test different meshes

Although τ_{LR} times are different among different mesh models, fully developed VDEs seem quite independent of these models

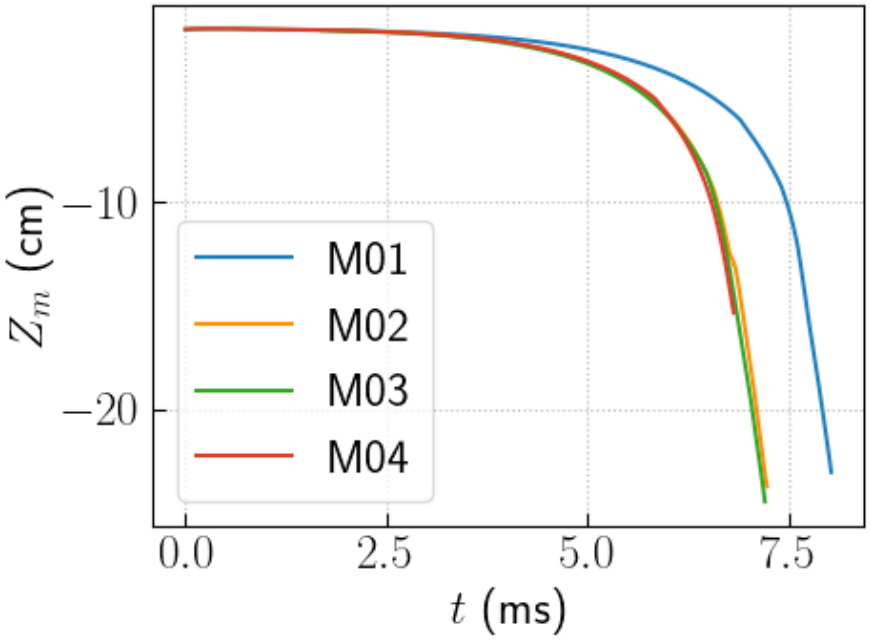

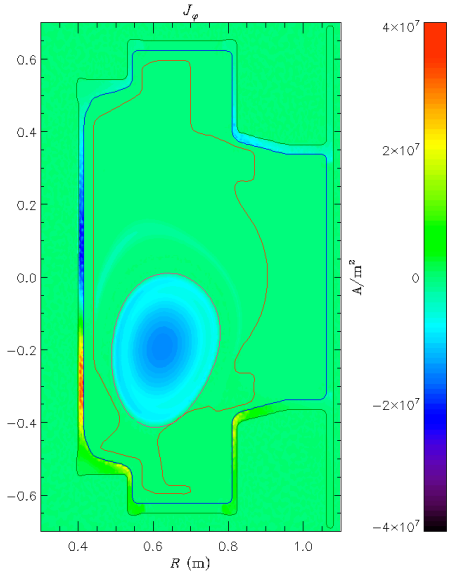

Most induced currents occur in the inner VV

Thermal conductivity ($\kappa_\perp$) influences the Vertical Displacement up/down motion

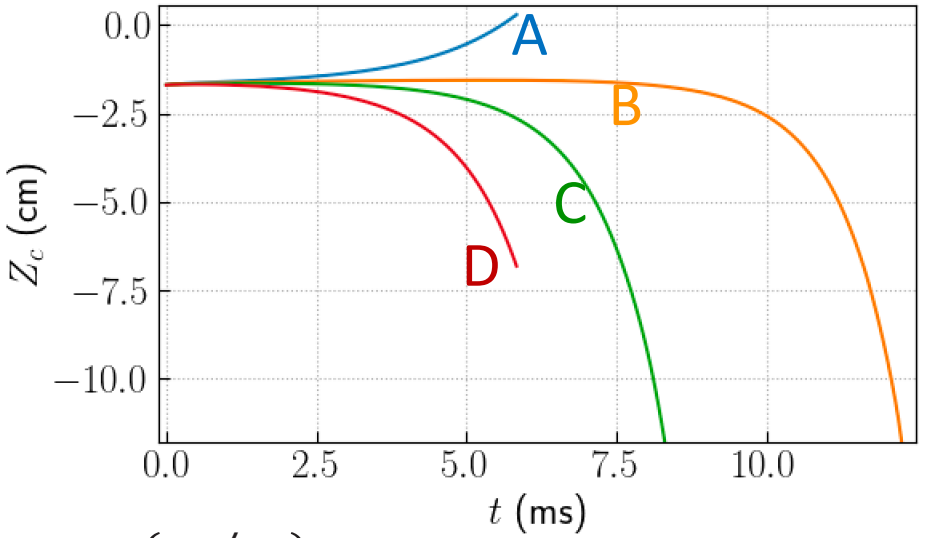

$(\kappa_\perp/n_0)$

A: $\sim 1.0\ \mathrm{m^2/s}$

B: $\sim 1.6\ \mathrm{m^2/s}$

C: $\sim 2.0\ \mathrm{m^2/s}$

D: $\sim 4.0\ \mathrm{m^2/s}$

Initial current density

$\Delta t\ =\ 1.2$ ms

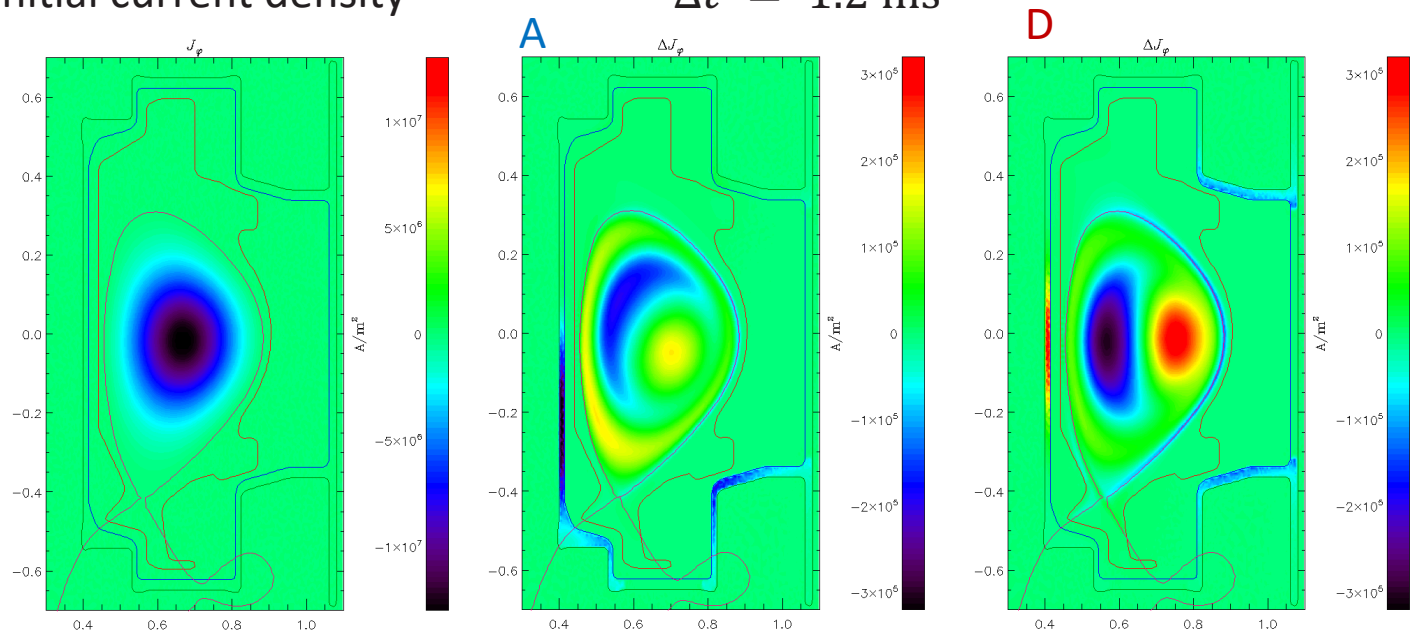

Fully developed downward VDE becomes independent of this choice

VDE evolved until edge safety factor fell below 2 without forcing a thermal quench

(CM-440-m04-01)

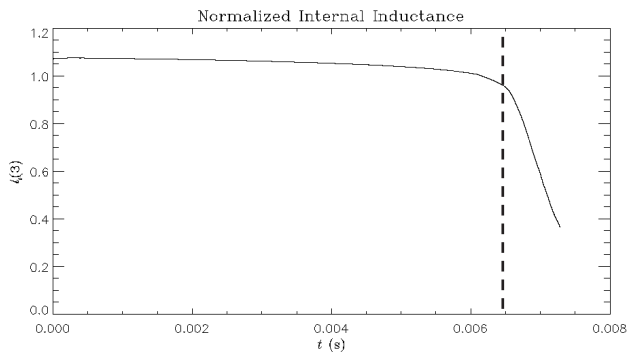

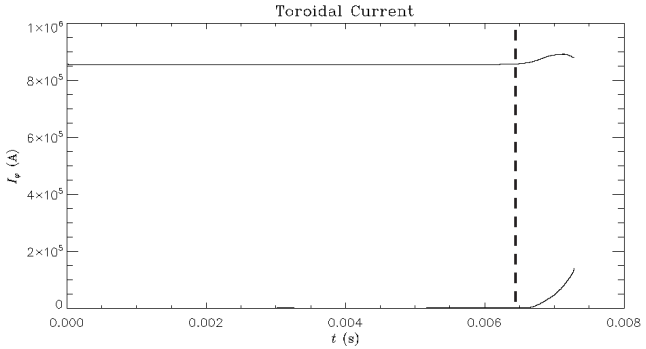

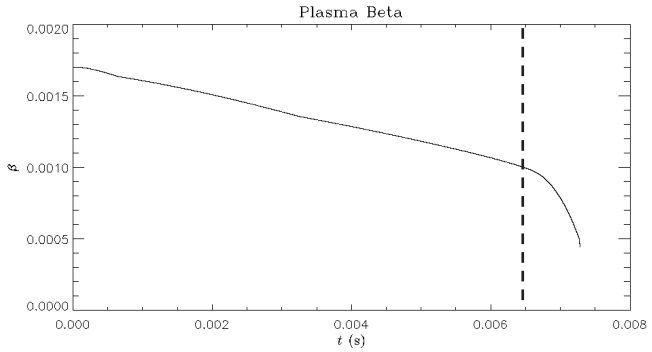

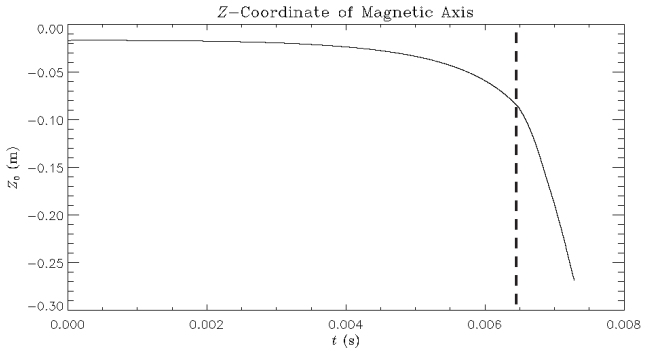

currents spike occurs due to a reduction of the inductance after wall contact

Scans over poloidal wall resistivity

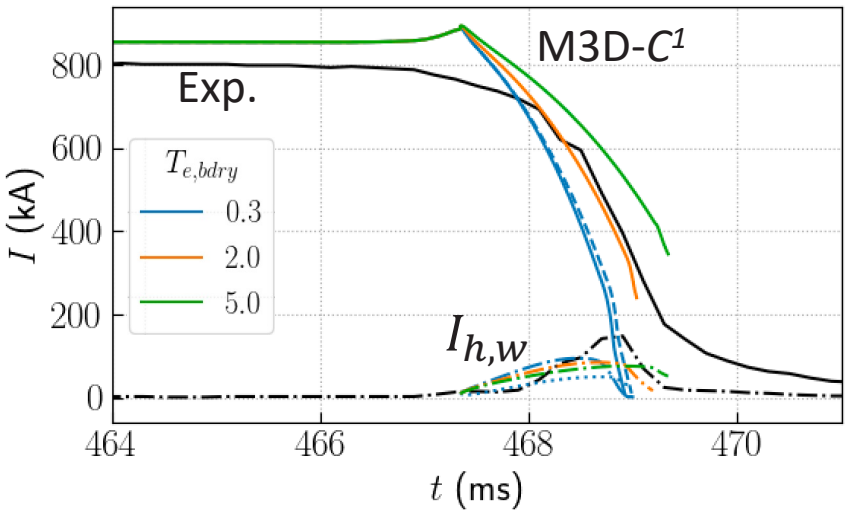

1e-5

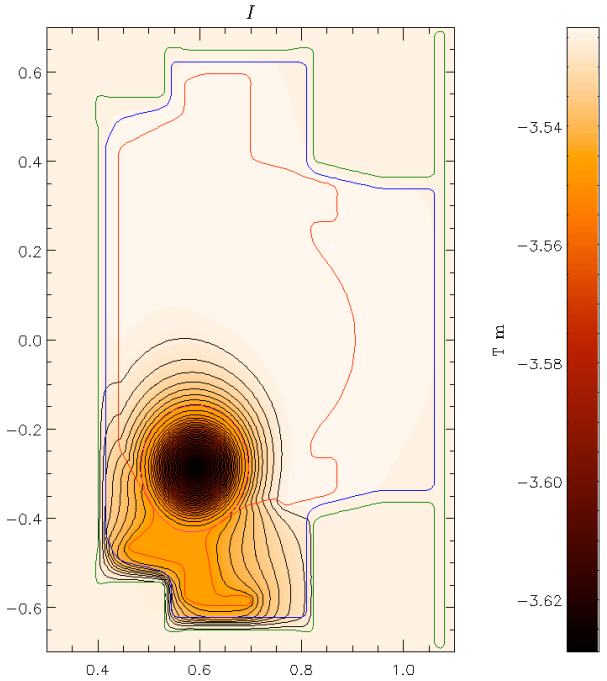

1e-3

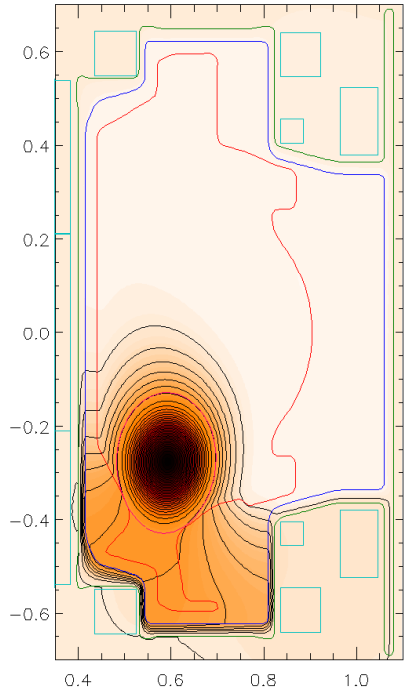

Increasing boundary (halo region) temperature changes the VDE rate

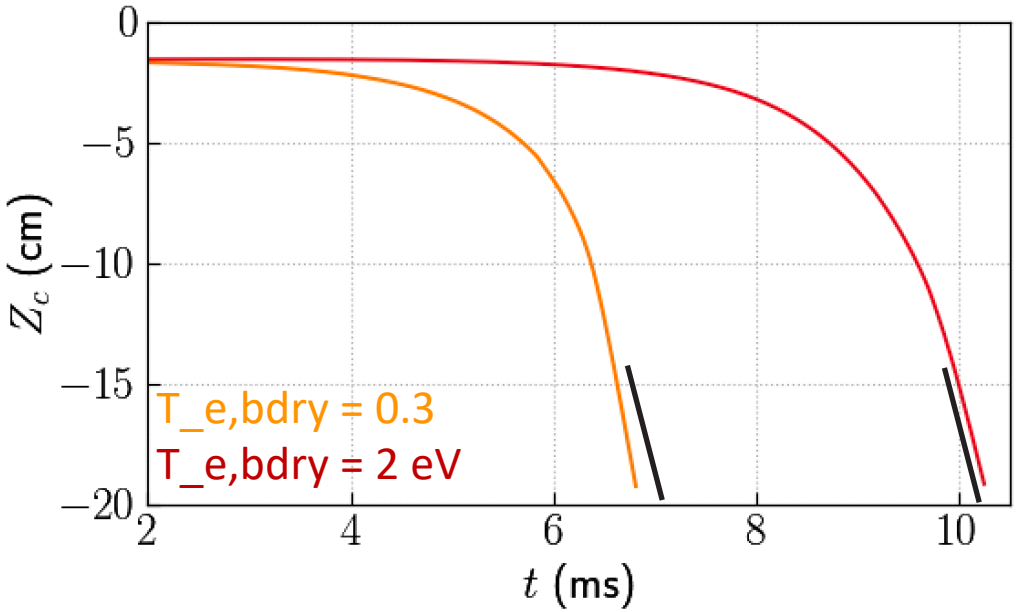

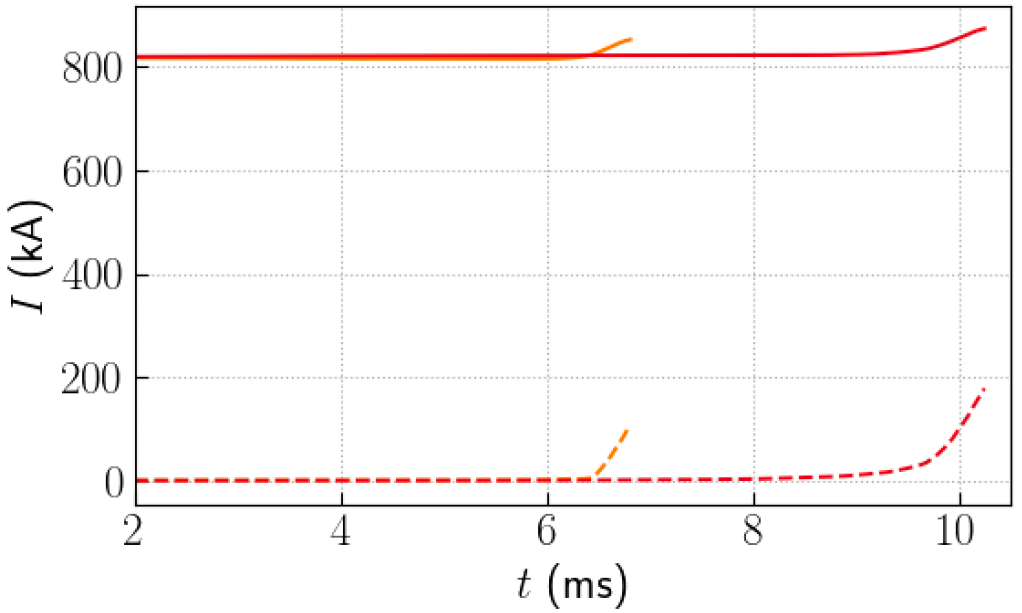

M3D-C1 is an X-MHD code that include resistive walls and other disruption-relevant capabilities

$$\frac{\partial n_s}{\partial t} + \nabla \cdot (n_s \mathbf{u}) = \sigma_s + \nabla \cdot (D_s \nabla n_s) \qquad s \in \{i, I_0, I_1, \ldots, I_Z\}$$

$$\rho\left(\frac{\partial \mathbf{u}}{\partial t} + \mathbf{u} \cdot \nabla \mathbf{u}\right) = \mathbf{J}\times\mathbf{B} - \nabla p - \nabla \cdot \Pi$$

$$n_e\left(\frac{\partial T_e}{\partial t} + \mathbf{u} \cdot \nabla T_e + (\Gamma - 1) T_e \nabla \cdot \mathbf{u}\right) + \sigma_e\, T_e = (\Gamma - 1)(Q_e + Q_{rad} + Q_\Delta + \nabla \cdot \mathbf{q}_e + \eta J^2 + \cdots)$$

$$n_I\left(\frac{\partial T_i}{\partial t} + \mathbf{u} \cdot \nabla T_i + (\Gamma - 1) T_i \nabla \cdot \mathbf{u}\right) + \sigma_I\, T_i = (\Gamma - 1)(Q_I - Q_\Delta + \nabla \cdot \mathbf{q}_I + \Pi_I : \nabla \mathbf{u} + \eta J^2)$$

$$\frac{\partial \mathbf{B}}{\partial t} = \nabla\times\left(\mathbf{u}\times\mathbf{B} - \eta(\mathbf{J} - \mathbf{J_{RE}}) - \frac{1}{n_e e}[\mathbf{J}\times\mathbf{B} - \nabla p_e]\right)$$

$$\mathbf{J} = \nabla\times\mathbf{B}$$

$$\Pi_i = \Pi_i^{\parallel} + \Pi_i^{\wedge} + \Pi_i^{\perp}$$

$$\mathbf{q}_s = -\kappa\, \nabla \mathrm{T_s} - \kappa_{\parallel} \hat{\mathbf{b}}\hat{\mathbf{b}} \cdot \nabla \mathrm{T_s}$$

$$\rho = m_i n_i + \sum_{z=1}^{Z} m_Z n_z$$

$$n_e = Z_i n_i + \sum_{z=1}^{Z} z\, n_z$$

$$n_I = n_i + \sum_z n_z$$

$$\sigma_e = Z_i \sigma_i + \sum_{z=1}^{Z} z\, \sigma_z$$

$$\sigma_I = \sigma_i + \sum_z \sigma_z$$

$$\frac{\partial n_{RE}}{\partial t} + \nabla \cdot (n_{RE} \mathbf{u}_{RE}) = \sigma_{RE}$$

$$\mathbf{u}_{RE} = c\, \mathbf{b} + \frac{\mathbf{E}\times\mathbf{B}}{B^2}$$

$$\mathbf{J}_{RE} = -n_{RE} e\, \mathbf{u}_{RE}$$

- Compressible, resistive MHD with single impurity species
- All charge state densities for single impurity species are evolved separately
- All ions (main & impurities) assumed to have same temperature T_i
- Separate equations for T_e and T_i since electrons lose heat much faster than ions during mitigation
- Fluid Runaway Electron model evolved self-consistently with MHD equations
- PIC ion model also now implemented [Liu, *et al. Comp. Phys. Comm.* **275**, 108313 (2022)]

NM Ferraro - APS-DPP - Oct 30, 2023